JACS
JOURNAL OF THE AMERICAN CHEMICAL SOCIETY

ARTICLE

pubs.acs.org/JACS

Axial Structure of the Pd(II) Aqua Ion in Solution

Daniel T. Bowron,[†] Elizabeth C. Beret,[‡,∥] Eloisa Martin-Zamora,[§] Alan K. Soper,[†] and Enrique Sánchez Marcos*[,‡]

[†]ISIS Facility, Rutherford Appleton Laboratory, Harwell Science and Innovation Campus, Didcot OX11 0QX, United Kingdom
[‡]Departamento de Química Física and [§]Departamento de Química Orgánica, Universidad de Sevilla, 41012-Sevilla, Spain

Supporting Information

ABSTRACT: Solution chemistry of Pd(II) and Pt(II) complexes is relevant to many fields of chemistry given the widespread applications of their compounds in homogeneous and heterogeneous catalysis, intermediate reaction synthesis, and antitumoral drugs. The well-defined square-planar arrangement of their complexes contrasts with the rather diffuse axial environment in solution. A theoretical proposal for a characteristic hydration shell in this axial region, called the meso-shell, stimulated further experimental and theoretical studies which have led to different pictures. The present work characterizes the structure of the axial region of the Pd(II) aqua ion in solution using a combination of neutron and X-ray diffraction and extended X-ray absorption fine structure (EXAFS) spectroscopy, with empirical potential structure refinement (EPSR). The results confirm the existence of the axial region and structurally characterize the water molecules within it. An important finding not previously reported is that the counterion, in this case the perchlorate anion, competes with water molecules for the meso-shell occupancy. The important role played by the axial region in many ligand substitution reactions is therefore intimately connected with the presence of the counterion and not just hydration water. This must call the attention of the experimental community to the important role that the counterion of the precursor salt must play in the synthesis.

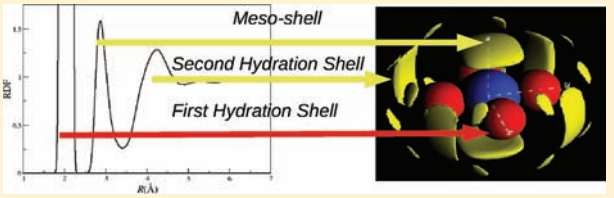

1. INTRODUCTION

Coordination chemistry of Pd(II) and Pt(II) is ruled by their d^8 electronic configuration. This explains the usual square-planar ligand arrangement around these two transition-metal cations. Their aqueous solutions are then primarily conditioned by tetrahydrates forming well-defined square-planar aqua ions. The solution chemistry of these cations has attracted experimental and theoretical attention because of their relevance in catalytic processes[1−3] and the pharmacological activity of some derivatives in several cancer treatments.[4,5] Reaction mechanisms of Pd(II) and Pt(II) complexes in aqueous solution have often been associated with entering and releasing of ligands or water molecules involving the axial regions.[6,7] This leads us to focus attention on how the Pd(II) and Pt(II) hydration structure must be envisaged.

In 1945, Frank and Evans[8] suggested that the strong electrostatic interactions due to the charge borne by metal cations induce in water a series of concentric shells which are responsible for their hydration. Except for some cases of highly charged metal cations, where a third shell may be invoked, it is usually accepted that only two hydration shells are well-defined and that beyond them bulk water properties are recovered. A further step of this model recognizes that the strong interactions among the bare cation and the first-shell water molecules make them distinct from the bulk molecules. First-shell water molecules could then be envisaged like ligands intimately joined to highly charged metal cations, that leads to the aqua ion concept, $[M(H_2O)_n]^{m+}$.[9,10] Many transition-metal cations form highly symmetric coordination compounds that fit well Frank and Evans's model. However, for the square-planar Pd(II) and Pt(II) aqua ions, the concentric shell model must be revisited by addressing the question of how the hydration structure in the regions above and below the molecular plane are defined.[11,12]

Pioneering wide angle X-ray scattering (WAXS)[6,13] and extended X-ray absorption fine structure (EXAFS)[14] studies on the hydration structure of the Pt(II) did not find evidence of axial water molecules. The first report on the hydration structure in this region was given by Martinez et al.,[15] based on classical molecular dynamics (MD) simulations of a highly diluted Pd(II) aqueous solution; a new hydration shell in the axial regions was revealed in the Pd−O and Pd−H radial distribution functions (RDF). The water molecules in this region show structural and dynamical properties noticeably different from those of the first and second shell, with the ensemble of their properties being a compromise among first and second shell, and even the bulk. This compelled Martinez et al.[15] to propose the term *meso-shell* for this hydration type; this new term aims to stress that water molecule behavior in this axial region may no longer be identified with the first or the second hydration shell. A later classical MD study of the Pt(II)[16] case gave evidence for a less tightly bound meso-shell at ∼3 Å, indicating that the structural and dynamical disorder of

Received: July 11, 2011
Published: August 10, 2011

these water molecules will not allow their detection by EXAFS. After this proposal, experimental and theoretical studies have addressed the question of the nature of the hydration shell of both cations as well as other related complexes in aqueous solutions.

Purans et al.[17] assigned a weak hump in the Pd K-edge EXAFS spectrum of an acid aqueous solution of $Pd(NO_3)_2$ to one or two water molecules at a distance of 2.50 Å, whereas Hofer et al.[18] extracted from the EXAFS function a shell at ~2.72 Å which was ascribed to two water molecules forming a weak bond with the metal. This led these authors to identify this arrangement as something similar to the structures resulting from a Jahn−Teller effect. However, the EXAFS fitting to square-pyramidal orientation, giving a distance of 2.81 Å, was also compatible with the EXAFS spectrum. These authors supported the presence of axial water molecules by means of quantum mechanics/molecular mechanics hybrid MD simulations, predicting a distance of 2.7 Å.[18] Beret and co-workers[19,20] found a more elusive axial hydration water molecules for both Pd(II) and Pt(II) aqua ions by means of CPMD simulations. For the Pt(II) case, the proposal of an asymmetric behavior was given, predicting a rather unexpected hydrogen bonding of one of the axial water molecules with the Pt cation. This unusual arrangement, particularly in the cationic and neutral complexes, has been called "anionic"[19,20] or "inverse"[21,22] hydration mode.

Further experimental and theoretical studies of Pt(II) aqueous solutions have supplied different qualitative and quantitative descriptions on the number and relative orientations of the axial water molecules.[21−29] The different quantitative and qualitative results derived from the different techniques reflect the rather elusive character of the axial hydration shell. This might also be joined to the probably different behavior of the two metal cations. The present work addresses the question of the experimental detection of the water molecules contributing to the hydration structure in the axial region of the Pd(II) aqua ion by undertaking a recently proposed multechnique approach which is particularly appropriate for this demanding problem.[30] A set of neutron and X-ray diffraction measurements, combined with a modified reverse Monte Carlo method, the empirical potential structure refinement (EPSR) method,[31] applying constraints on the local order around the metal cation by means of information derived from the corresponding EXAFS spectrum,[32] have been performed. The ensemble of these techniques, which are able to provide with different weights the structural information on different regions around the central cation, seems particularly suitable to explore this controversial problem. Thus, EXAFS informs on the local order around the Pd cation, whereas neutron diffraction provides the whole water structure and its changes in the presence of the aqua ion. The X-ray diffraction pattern, although also being sensitive to the global solution structure, increases preferentially its sensitivity to the patterns involving the heavy metal cation.[33]

2. METHODS

Three 0.425 M aqueous solutions of Pd(II) acetate in 1.25 M $HClO_4$ acid to prevent hydrolysis of the aqua ion were prepared from p.a. Sigma-Aldrich reactant (ref 520764) in H_2O, in D_2O, and in an equimolar H_2O-D_2O mixture, HDO. Neutron scattering measurements were carried out at room temperature at the ISIS pulsed neutron source of the Rutherford Appleton Laboratory (U.K.) on the SANDALS instrument. This is specially optimized for the study of liquid samples containing hydrogen. Additional X-ray data for the aqueous solution of palladium acetate in H_2O have been collected on a PANalytical XPERT-PRO $\theta/2\theta$ diffractometer using silver radiation (Kα = 0.5594 Å). The experimental setup for the liquid sample measurements was similar to that employed in recent measurements of other solutions.[30,34] The standard corrections and normalizations have been applied to the neutron and X-ray data by means of the suite of programs Gudrun and GudrunX, respectively.[35] To refine the information about the Pd(II) aqua ion structure, the average of three Pd K-edge XAS spectra of a 0.1 M aqueous solution of Pd(II) nitrate in 1 M $HClO_4$ acid, recorded in absorption mode at the Synchrotron Radiation Source (ESRF, Grenoble, France). The BM29 beamline, was used. Standard procedures for the EXAFS signal extraction from the spectrum were applied as detailed elsewhere.[36]

The extraction of the real-space pair-distribution functions from the structure factors obtained from neutron and X-ray scattering diffractograms needs their decomposition into a linear combination of partial structure factors. This task has been undertaken by means of data modeling based on the EPSR approach.[31] The method is based on a classical NVT Monte Carlo simulation of the system under study which employs an iterative algorithm to achieve consistency between the experimental scattering data and model functions derived from the statistically simulated system. The initial stage of the procedure consists of a thermalization of the simulation system by using a set of reference interparticle potentials. These initial potentials are modified by adding empirical terms in an iterative manner to minimize the residual function between the experimental and computed structure factors. Details of the procedure can be found elsewhere.[30,31,34]The SPC/E model was adopted for the water molecules. A table with the Lennard−Jones and charge parameters for the different species employed to build the reference potential is given in the Supporting Information (Table S1). The simulation box was formed by 20 palladium cations, 40 acetic acid molecules, 59 perchlorate anions, 19 protons (treated as soft charged spheres), and 2281 water molecules. The simulated molecular ratios are the same as the experimental ratios, considering that, due to the acid concentration provided by the perchloric acid, the acetate anion is in its protonated form.

In order to improve the initial description of the model system, we have assumed that the metal cation in this solution is in its aqua ion form, that is, the square-planar $[Pd(H_2O)_4]^{2+}$.[10] The statistical incorporation of the hydrated ion concept has already been applied for Pd(II) and Pt(II) aqueous solution,[15,16] leading to satisfactory descriptions of their solution properties. In this case, the method applied to incorporate the flexibility of the aqua ion has been similar to that previously employed for Cr^{3+}.[30]

3. RESULTS AND DISCUSSION

Figure 1 shows the neutron and X-ray data together with the fitted data obtained by the EPSR model and their corresponding residuals. The agreement of the simulated structure factors is good in all cases. It must be noted that a common atomistic representation provided by the MC simulation using the final refined intermolecular potentials is able to simultaneously match the structure of the three different solutions and four different diffractograms. The top of Figure 1 shows the comparison of the experimental and simulated k^2-weighted EXAFS spectrum for the Pd(II) aqueous solution. The simulated EXAFS spectrum was obtained by averaging the individual spectra that result from selecting 10 000 local structures from the same MC simulation. The FEFF (version 8.4) code[37] has been employed to simulate the spectrum for each structure. An example FEFF input file is given in the Supporting Information. Good agreement between the experimental and simulated spectra is observed. The EXAFS oscillation is mainly dominated by the contribution of the scattering paths including the oxygen atoms of the water

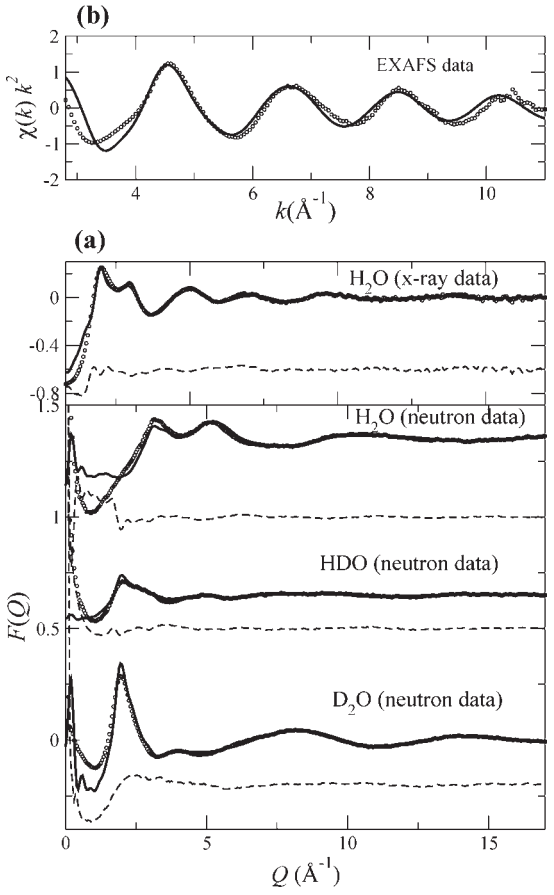

Figure 1. Experimental and fitted neutron and X-ray diffraction data and experimental and simulated EXAFS spectrum for different Pd(II) aqueous solution. (a) X-ray and neutron data of palladium acetate acid aqueous solutions in H_2O, D_2O, and HDO: experimental (dots), EPSR model fits (solid lines), and fit residuals (dashed lines). (b) Pd K-edge k^2-weighed EXAFS data of a Pd(II) nitrate acid aqueous solution in H_2O: experimental spectrum (dots) and simulated spectrum (solid line) from snapshots provided by the EPSR simulation.

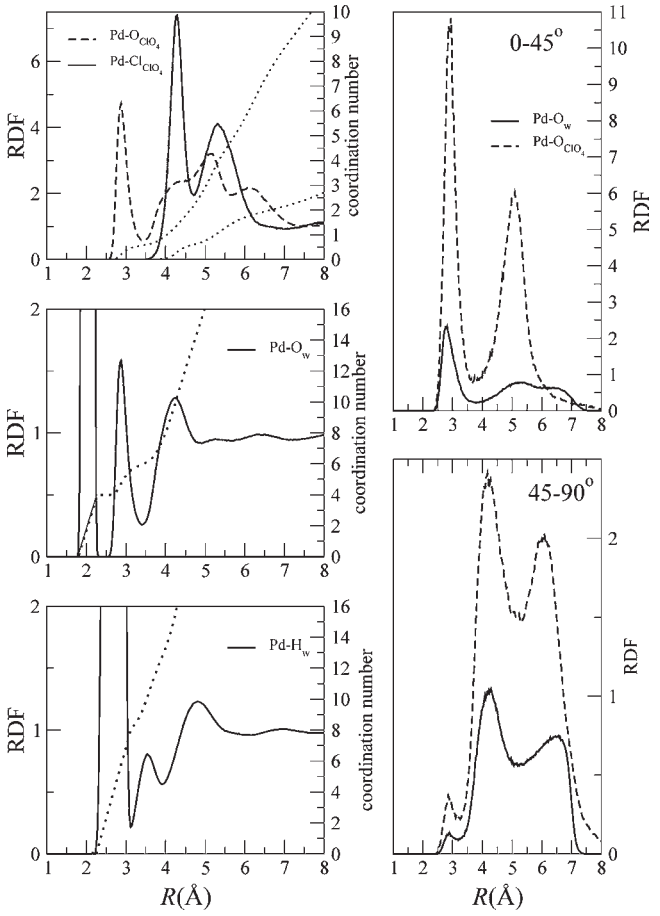

Figure 2. Left: Pd−X pair RDF (solid and dashed lines) and running coordination numbers (dotted lines). Right: Pair partial RDF for the axial and equatorial regions. Left: Pd−H (bottom), Pd−O (middle), Pd−$O_{ClO_4^-}$ (top, dashed line), and Pd−$Cl_{ClO_4^-}$ (top, solid line) RDFs obtained from the EPSR simulation. (left y-axis corresponds to $g(r)$; right y-axis corresponds to running coordination numbers). Right: Partial Pd−O and Pd−$O_{ClO_4^-}$ RDFs corresponding to the axial (0−45°) and the equatorial (45−90°) region. (the partial Pd−O_w RDFs have been built excluding the first-shell water molecules.)

molecules forming the Pd(II) tetrahydrate. The tetrahydrate was represented in the EPSR simulation as a molecule containing a Pd atom at its center surrounded by four water molecules placed in a square-planar arrangement. The EXAFS data were not included in the EPSR procedure for refining the potential, but the reference potential parameters of the Pd aqua ion used in EPSR simulation were refined against the EXAFS data to give agreement in phase and intensity of the simulated spectrum.[32,33]

Figure 2 collects the most relevant pair distribution functions of the EPSR model that fit the experimental data. The Pd−O_w RDF shows a first sharp peak centered at 2.04 Å that integrates to 4 oxygen atoms which belongs to the Pd aqua ion. This value agrees with the range of previous values provided in the literature [2.00−2.04 Å].[15,17−20] A second less intense but well-defined peak centered at 2.85 Å integrates to ∼2 oxygen atoms confirms the axial hydration, which encloses a distance range distribution of 2.7−3.5 Å. These values for the axial coordination are close to the theoretical values predicted by Martinez et al.[15] and Hofer et al.[18] of 2.7−2.8 Å, but are larger than the EXAFS-based value proposed by Purans et al.[17] of 2.5 Å. A third broader peak extended from ∼3.6−4.8 Å, centered at 4.2 Å and integrating to 8 oxygen atoms, contains the equatorial second hydration shell. This second hydration shell peak gives a value similar to that given by Martinez et al.[15] of 4.1 Å, but is shorter than the one estimated by Hofer et al.[18] of 4.4 Å. The minimum of the Pd−O_w peak corresponding to the axial coordination does not go down to zero. This indicates that water molecules in the meso-shell easily exchange with bulk. This fact agrees with the difficulties to distinguish between an associative activation Interchange (I_a) and an associative (A) mechanism for the water-exchange process in the $[Pd(H_2O)_4]^{2+}$ aqua ion.[7,38] The Pd−H_w RDF provides a set of three peaks consistent with the Pd−O_w RDF, shifted with respect to the oxygen correlations at such distances that indicate that an ion−water dipole orientation is adopted by water molecules surrounding the Pd(II) cation. It is worth noting that this global behavior rules out the possibility of an anionic hydration in the axial region, as has been proposed for the Pt hydration case.[21,20] The third plotted RDFs correspond to the distributions of the perchlorate atoms around the metal cation. It is noticeable that the first Pd−$O_{ClO_4^-}$ peak is centered at the same position as the second Pd−O_w peak, and their widths are also similar. Both peaks present the same topology, except for

their heights. The perchlorate feature is more than two times higher than that of water and is equally well-defined. This is expected due to the preferential attractive character that the metal cation aqua ion induces in its closest environment for anions, compared with the water molecules playing the solvent role, as well as the relative concentration of anions with respect to water. In fact, the running coordination number is 0.5 oxygen atoms. This close similarity indicates that the regions above and below the molecular plane of the aqua ion can be envisaged not only as a hydration shell but also as a coordination region. Thus, a polyoxoanion, such as perchlorate, is a molecularly well-fitted coordinating molecule which may be playing a similar role to that of the water molecules in this region.

The first peak of the Pd−$Cl_{ClO_4^-}$ RDF is centered at ∼4.25 Å, that is, shifted about 1.40 Å with respect to the position of the first maximum of the Pd−$O_{ClO_4^-}$ RDF, and it integrates to the same value of 0.5. The Cl−O bond length in the perchlorate anion is 1.47 Å. These data indicate that the average orientation of the perchlorate anion in the axial region is generally pointing only one of its oxygen atoms toward the metal cation. The second broad peak of the Pd−$Cl_{ClO_4^-}$ RDF, centered at ∼5.30 Å, integrates to ∼1 chloride atom. It corresponds to chloride atoms belonging to the anions coordinating the equatorial water molecules. In the light of the perchlorate Cl distributions, the broad Pd−$O_{ClO_4^-}$ distribution extending from 3.8 to 6.8 Å is the overlapping result of the peaks corresponding to the rest of the oxygen atoms belonging to the axial perchlorate anion (peak at ∼5.2 Å) and those belonging to the equatorial region: the first hump at ∼4.2 Å corresponds to the perchlorate oxygen atoms forming the hydrogen bonding, whereas the broad third peak at 6.2 Å corresponds to the outer oxygen atoms of the equatorial perchlorate anions.

When the solute under study presents a relevant symmetry element, as in the Pd(II) aqua ion case, a decomposition of the total RDF, in partial RDFs, with each of them corresponding to excluding regions of the space, can be performed.[19] Two partial RDFs corresponding to the axial (0−45° range of the azimuthal angle) and the equatorial regions (45−90°) for Pd−O_w and Pd−$O_{ClO_4^-}$ have been included in Figure 2. It is worth pointing out that these partial RDFs have included all the oxygen atoms beyond a Pd−O_w cutoff radius of 2.5 Å, namely the oxygen atom first-shell is excluded for clarity reasons. These plots support the structural analysis carried out previously. The Pd−O_w peak at 2.85 Å appears in the axial partial RDF (0−45°), whereas the peak at ∼4.2 Å appears in the equatorial partial RDF (45−90°). In the axial Pd−$O_{ClO_4^-}$ partial RDF, a peak at 2.85 Å is seen for the perchlorate oxygen coordinating the Pd and a second peak at ∼5 Å belonging to the rest of oxygens of the axial perchlorate anion. The equatorial Pd−$O_{ClO_4^-}$ partial RDF contains the two peaks centered at 4.0 and 6.0 Å for oxygen atoms belonging to the perchlorate anions occupying the equatorial region.

Spatial distribution functions[39] (SDFs) provide a complementary 3D view of the structure surrounding the Pd aqua ion by defining isochoric surfaces which show the highest probability regions for finding a given species. Figure 3 shows SDFs for the center of mass of water molecules (top) and perchlorate anions (bottom). For the water SDF, the yellow surfaces show that the equatorial region is formed by four banana-shaped lobes occupying the intermediate regions between the Pd−O_I bonds. This shape is imposed by the hydrogen bonds formed with the first-shell water molecules, whose librational and rotational movements mainly affect their hydrogen atoms. A second region that is

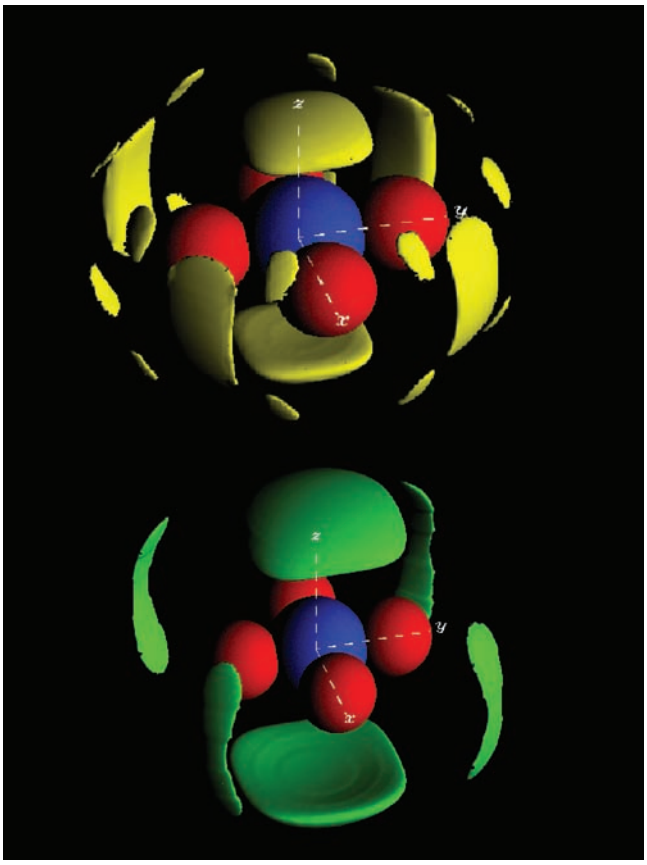

Figure 3. Spatial distribution functions around the Pd(II) aqua ion. Pd cation (blue sphere), oxygen atoms of the aqua ion (red spheres). Top, water oxygen atoms (yellow surfaces); bottom, perchlorate chlorine atoms (green surfaces).

well-defined in the SDF corresponds to the lobes above and below the molecular plane which form the axial hydration region. The extent of the region indicates that these water molecules although much closer to the metal cation (the corresponding maximum RDF peak is at 2.85 Å) than the second hydration shell (the corresponding maximum RDF peak is 4.2 at Å) smear much more than the water molecules of the first shell, so that their pattern is rather intermediate between that of the first and the second shell. This finding represents an experimental support of the meso-shell concept.[15] It is also interesting to note the set of small lobes in between the equatorial and the axial regions. These small spots are due to water molecules which are bridging the equatorial second hydration shell with the axial region. These bridge water molecules are a consequence of the high ability of bulk structure to fit the molecular shape of the solute, establishing a hydrogen bond network which helps to support the meso-shell. This bridge region had been already observed in the classical MD simulation of Pd(II) carried out by Martinez et al.[15]

The SDF corresponding to the perchlorate anion around the Pd(II) aqua ion is shown in the bottom of Figure 3 (green surfaces). It is interesting to point out how similar its axial distribution is to that of the water. This reinforces the finding, already observed in their corresponding RDFs, concerning the similar axial coordination pattern adopted by water molecules and the counterions of polyoxoanionic nature. This similarity must be understood on the basis of the combination of an

attractive molecular cation, the square-planar Pd(II) aqua ion, providing an oblate-like molecular shape and the high molecular adaptability of the water structure.[40] The cooperative effects define attracting conical regions above and below the central cation that can accommodate preferentially hard donor ligands as water molecules or perchlorate anions. The equatorial region shows four lobes centered in the bisectrix region of the OPdO angle. These are the regions occupied by the first-shell hydrogen atoms which favor the hydrogen bond formation with anion oxygen atoms. As in the water case, the banana-shaped distribution is a consequence of the librational degrees of freedom of hydrogen atoms in the first hydration shell. It is worth noting that these 3D representations provide the spatial probabilities relative to the distribution of each species independently, that is, water molecules or perchlorate anions. Therefore, although their patterns are similar, particularly in the axial region, the water occupancy is more than 4 times that of the anion.

4. CONCLUDING REMARKS

The axial structure of the tetrahydrate Pd(II) in aqueous solution has been experimentally determined by the combined use of neutron and X-ray diffraction techniques, EXAFS, and an atomistic representation of the system based on a specially designed reverse Monte Carlo procedure, the EPSR method. The multitechnique approach including experimental methods specifically sensitive to the hydrogen atoms, the use of the hydrated ion concept in the atomistic model employed, and the EXAFS-refined description of the Pd(II) aqua ion have been keys to achieve an unambiguous experimental answer on the meso-shell detection.

The axial hydration is found to be centered at ∼2.85 Å containing on average two water molecules, each of them located on one side of the molecular plane. There is then an intermediate shell between the tightly bound water molecules of the first shell (2.04 Å) and the equatorial water molecules forming the second hydration shell (4.2 Å). These experimental results support the use of the theoretically proposed term, meso-shell.[15] This specific term emphasizes that structural and dynamical properties associated to the axial regions are different enough from those of the equatorial region, which accommodates the four tightly bonded water molecules forming the Pd aqua ion, namely, the first hydration shell.

However, some new fundamental insights have been achieved from the analysis of the present data. Experimental limitations force us to work with a nondilute aqueous solution and the presence of an acidic medium to prevent the hydrolysis of the $[Pd(H_2O)_4]^{2+}$ aqua ion. This was precluded in the theoretical MD simulation by the use of a nondissociable water model. As a result, the perchlorate anion distribution has been revealed to be significant in the close environment of the aqua ion, and in particular appears to display a similar axial coordination pattern to the aqua ion as adopted by the meso-shell water molecules. On one hand, this issue highlights that the meso-shell is not only a hydration structure but rather a coordination region built by the cooperative effects of the square-planar hydrated cation and the ability of water structure to fit around this to promote a particular interaction in the axial regions. In addition to water molecules, polyoxoanions, which share donor and topological properties with them, may be inserted. On the other hand, this axial anion coordination leads to the unexpected relevance that counterions may play in determining the chemical reactivity of square-planar metal complexes. Equatorial ligand substitution processes are usually proposed to be initiated by axially entering reactants.[3,7] It is usually thought that the initial step is a dehydration process that must be conditioned by the meso-shell characteristics. From the present results, these initial steps involving the axial region may also be affected by the presence of the counterion, charged species which may impose a different behavior on the entering reactant. This raises the chemical conclusion that, as a function of the counterion chosen for the metalo-precursor salt, the subsequent reaction mechanisms could be affected. In other words, the shared access to the meso-shell of both water and perchlorate anion, as a prototype of polyoxoanion, stresses the specific character of the anion role in the in-solution chemical reactivity. This specificity is going beyond the classical Brönsted−Bjerrum equation,[41,42] where the ion effects on chemical reactions are quantified by the ionic strength, that is, a measure of the free charge in the media, regardless the chemical nature of the ions. The results presented point to a specific effect which is not derived from the intrinsic chemical interaction of the anion salt and some reactants, but from the combination of the hydration structure and the involved reactants; that is a specific chemical effect based on a collective medium behavior.

We believe that in this work the concept of the meso-shell has been experimentally supported in a robust manner by coupling three different highly demanding experimental techniques to an atomistic theoretical approach. The studied sample was chosen to be the best compromise between experimental chemical requirements and a concentration low enough to approach the theoretical dilute solution conditions modeled by previous computer simulations. These peculiar conditions have allowed us to extend the meso-shell concept from the traditional hydration to the coordination of a representative polyoxoanion as the perchlorate. To our knowledge, this is the first experimental evidence on this concurrent behavior. This may open new approaches in the field of solution chemistry by calling particular attention to the specific effects that counterions may produce in the media where reactions occur.

■ ASSOCIATED CONTENT

Supporting Information. Table with the Lennard−Jones and charges parameters employed for the reference intermolecular potentials in the EPSR method, input FEFF file, and Fourier transform of the Pd K-edged EXAFS spectrum of $Pd(NO_3)_2$ in water are included. This material is available free of charge via the Internet at http://pubs.acs.org.

■ AUTHOR INFORMATION

Corresponding Author
sanchez@us.es

Present Addresses
[||]Theory Department, Fritz-Haber-Institut der Max-Planck-Gesellschaft, D-14195 Berlin-Dahlem, Germany.

■ ACKNOWLEDGMENT

We thank Prof. Dominik Marx, Bochüm University, for stimulating discussions. We thank the ISIS Pulsed Neutron and Muon Facility (RAL, U.K.) for access to neutron beamtime (SANDALS) and X-ray diffractometer on Project RB910175. We

thank ESRF (Grenoble, France) for beam allocation time (BM29, CH-1192). Spanish Ministry of Science and Innovation is acknowledged for financial support (CTQ2008-05277). E.S.M. thanks the Spanish Ministry of Science and Innovation for a grant of the mobility program "Salvador de Madariaga" during his stay at the Rutherford Appleton Laboratory (Didcot, U.K.).

REFERENCES

(1) Leininger, S.; Olenyuk, B.; Stang, P. J. *Chem. Rev.* **2000**, *100*, 853–907.
(2) Vicente, J.; Arcas, A. *Coord. Chem. Rev.* **2005**, *249*, 1135–1154.
(3) Zhao, G.-J.; Stang, P. J. *J. Chem. Theory Comput.* **2009**, *5*, 1955–1958.
(4) Rosenberg, B.; van Camp, L.; Trosko, J. E.; Mansour, V. H. *Nature* **1969**, *222*, 385.
(5) Jung, Y.; Lippard, S. J. *Chem. Rev.* **2007**, *107*, 1387–1407.
(6) Deeth, R. J.; Elding, L. *Inorg. Chem.* **1996**, *35*, 5019–5026.
(7) Helm, L.; Merbach, A. E. *Coord. Chem. Rev.* **1999**, *187*, 151–181.
(8) Frank, H. S.; Evans, M. W. *J. Chem. Phys.* **1945**, *13*, 507–532.
(9) Taube, H. *J. Phys. Chem.* **1954**, *58*, 523–528.
(10) Richens, D. T. *The Chemistry of Aqua Ions*; John Wiley: Chichester, 1997.
(11) Marcus, Y. *Ion Solvation*; Wiley: Chichester, 1986.
(12) Persson, I. *Pure Appl. Chem.* **2010**, *82*, 1901–1917.
(13) Hellquist, B.; Bengtsson, L.; Holmberg, B.; Hedman, B.; Persson, I.; Elding, L. I. *Acta Chem. Scand.* **1991**, *45*, 449–455.
(14) Ayala, R.; Sánchez Marcos, E.; Daz-Moreno, S.; Solé, V. A.; Muñoz-Páez, A. *J. Phys. Chem. B* **2001**, *105*, 7588–7593.
(15) Martínez, J. M.; Torrico, F.; Pappalardo, R. R.; Sánchez Marcos, E. *J. Phys. Chem. B* **2004**, *108*, 15851–15855.
(16) Torrico, F.; Pappalardo, R. R.; Sánchez Marcos, E.; Martínez, J. M. *Theor. Chem. Acc.* **2006**, *115*, 196–203.
(17) Purans, J.; Fourest, B.; Cannes, C.; Sladkov, V.; David, F.; Venault, L.; Lecomte, M. *J. Phys. Chem. B* **2005**, *109*, 11074–11082.
(18) Hofer, T.; Randolf, B. R.; Shah, S.; Rode, B.; Persson, I. *Chem. Phys. Lett.* **2007**, *445*, 193–197.
(19) Beret, E. C.; Martínez, J. M.; Pappalardo, R. R.; Sánchez Marcos, E.; Doltsinis, N. L.; Marx, D. *J. Chem. Theory Comput.* **2008**, *4*, 2108–2121.
(20) Beret, E. C.; Pappalardo, R. R.; Doltsinis, N. L.; Marx, D.; Sánchez Marcos, E. *ChemPhysChem* **2008**, *9*, 237–240.
(21) Kozelka, J.; Bergés, J.; Attias, R.; Fraitag, J. *Angew. Chem., Int. Ed.* **2000**, *39*, 198–201.
(22) Rizzato, S.; Bergés, J.; Mason, S.; Albinati, A.; Kozelka, J. *Angew. Chem., Int. Ed.* **2010**, *49*, 7440–7443.
(23) Jalilehvand, F.; Laffin, L. *Inorg. Chem.* **2008**, *47*, 3248–3254.
(24) Hofer, T.; Randolf, B. R.; Rode, B.; Persson, I. *Dalton Trans.* **2009**, 1512–1515.
(25) Kocsis, L.; Mink, J.; Jalilehvand, F.; Laffin, L.; Berkesi, O.; Hajba, L. *J. Raman Spectrosc.* **2009**, *40*, 481–490.
(26) Stirling, A.; I. Bakó, L. K.; Hajba, L.; Mink, J. *Int. J. Quantum Chem.* **2009**, *109*, 2591–2598.
(27) Vidossich, P.; Ortuño, M.; Ujaque, G.; Lledós, A. *ChemPhysChem* **2011**, *12*, 1666–1668.
(28) Truflandier, L. A.; Autschbach, J. *J. Am. Chem. Soc.* **2010**, *132*, 3472–3483.
(29) Truflandier, L. A.; Sutter, K.; Autschbach, J. *Inorg. Chem.* **2011**, *50*, 1723–1732.
(30) Bowron, D. T.; Daz-Moreno, S. *J. Phys. Chem. B* **2009**, *113*, 11858–11864.
(31) Soper, A. K. *Phys. Rev. B* **2005**, *72*, 104204.
(32) Bowron, D. T. *Pure Appl. Chem.* **2008**, *80*, 1211–1227.
(33) Díaz-Moreno, S.; Ramos, S.; Bowron, D. T. *J. Phys. Chem. A* **2011**, *115*, 6575–6581.
(34) Imberti, S.; Bowron, D. T. *J. Phys.: Condens. Matter* **2010**, *22*, 404212.
(35) Soper, A. K. GudrunN and GudrunX. Programs for correcting raw neutron and x-ray diffraction data to differential scattering cross section. Rutherford Appleton Laboratory, Technical Report, RAL-TR-2011-013 (available online at http://epubs.stfc.ac.uk/work-details?w=56240), 2011.
(36) Merkling, P.; Muñoz-Páez, A.; Sánchez Marcos, E. *J. Am. Chem. Soc.* **2002**, *124*, 10911–10920.
(37) Ankudinov, A. L.; Ravel, B.; Rehr, J.; Conradson, S. *Phys. Rev. B* **1998**, *58*, 7565–7576.
(38) Helm, L.; Merbach, A. E. *Chem. Rev.* **2005**, *105*, 1923–1959.
(39) Svishchev, I. M.; Kusalik, P. G. *J. Chem. Phys.* **1993**, *99*, 3049–3058.
(40) Leberman, R.; Soper, A. K. *Nature* **1995**, *378*, 364–366.
(41) Bronsted, J. N. *Z. Phys. Chem.* **1925**, *115*, 337–364.
(42) Bjerrum, N. *Z. Phys. Chem.* **1925**, *118*, 251–254.